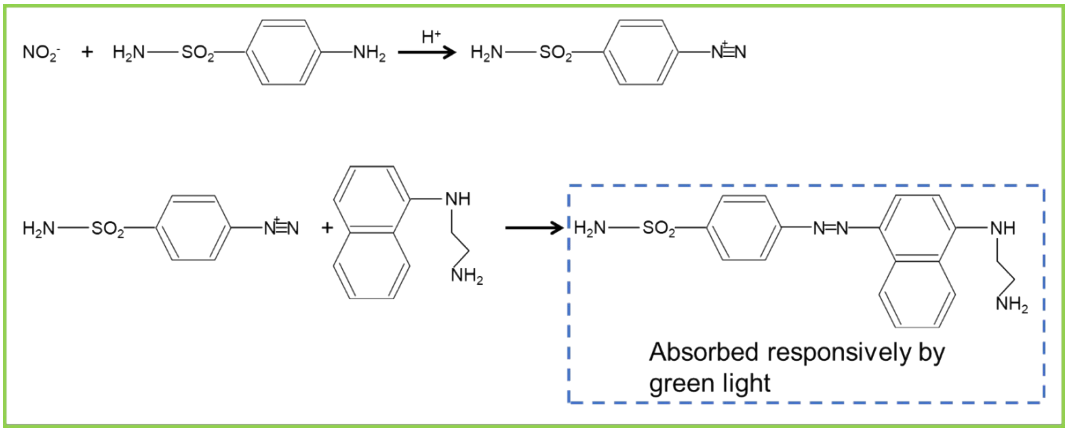

Figure S1. The principle of the Griess reaction used for detecting nitrites.

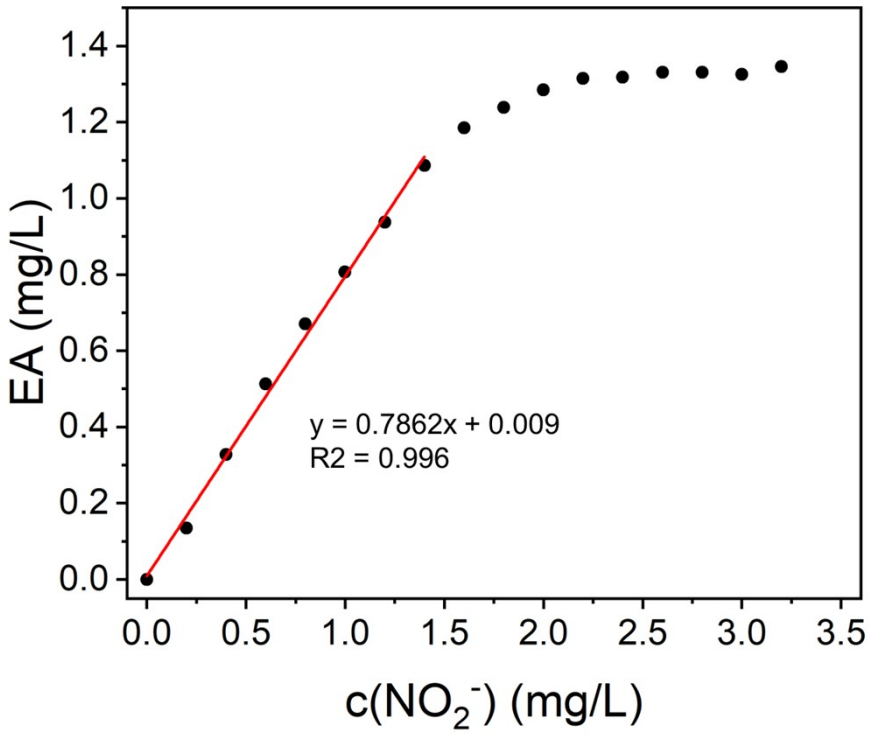

Figure S2. The linear detection range of the sensor.

Table S1. Standards for Detecting Nitrite Concentration

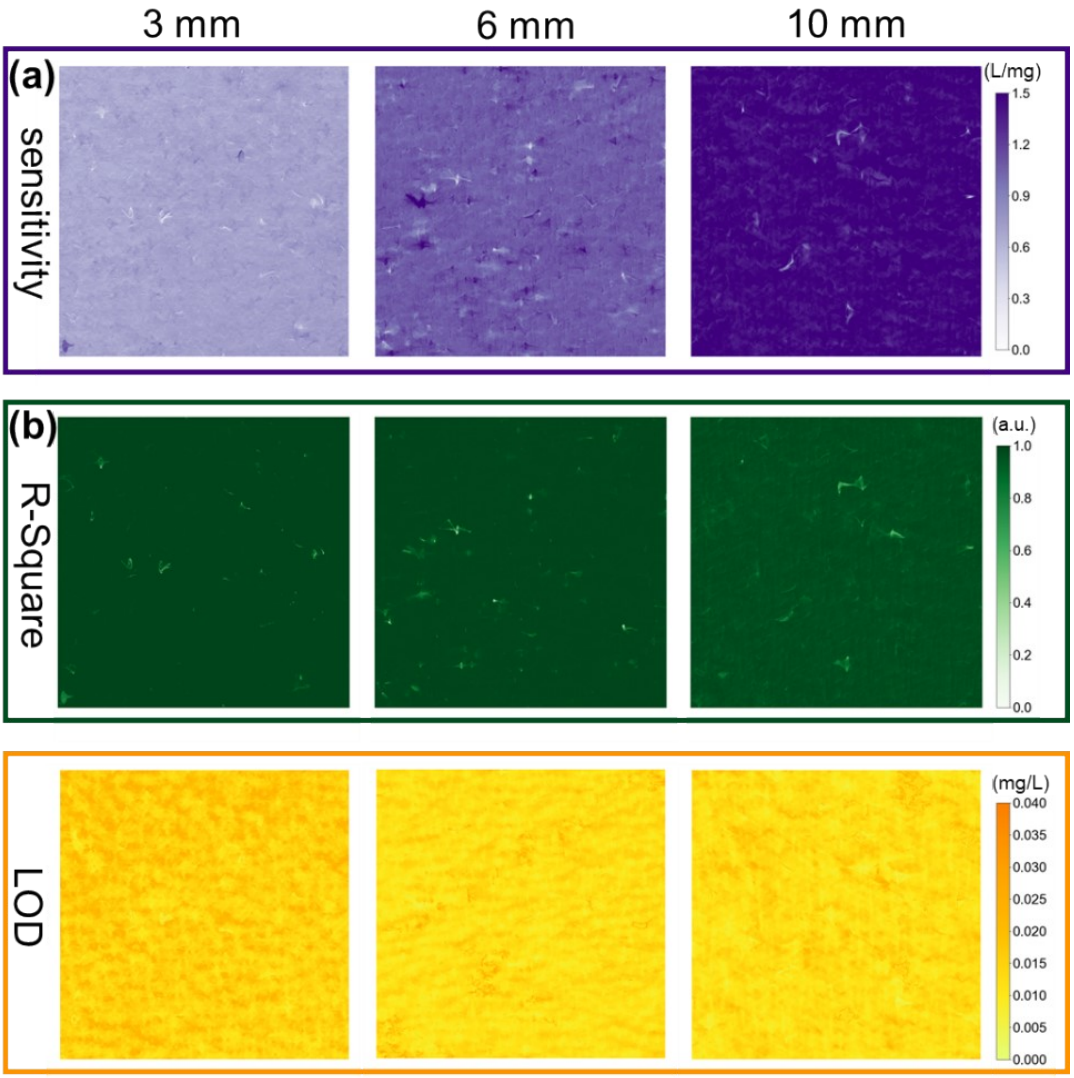

Figure S3. Calibration results for absorption modules with different absorption lengths (3mm, 6mm, 10mm). (a) Sensitivity distribution. (b) R-squared distribution. (c) Limit of Detection (LOD) distribution.

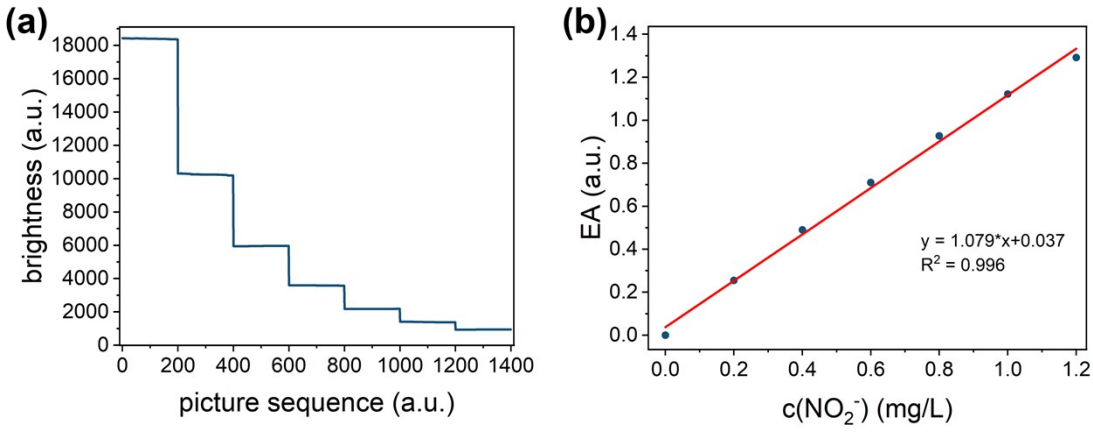

Figure S4. (a) Overall brightness corresponding to different nitrite concentrations (0, 0.2, 0.4, 0.6, 0.8, 1.0, 1.2 mg/L). (b) Linear fitting of overall equivalent absorbance against nitrite concentration.

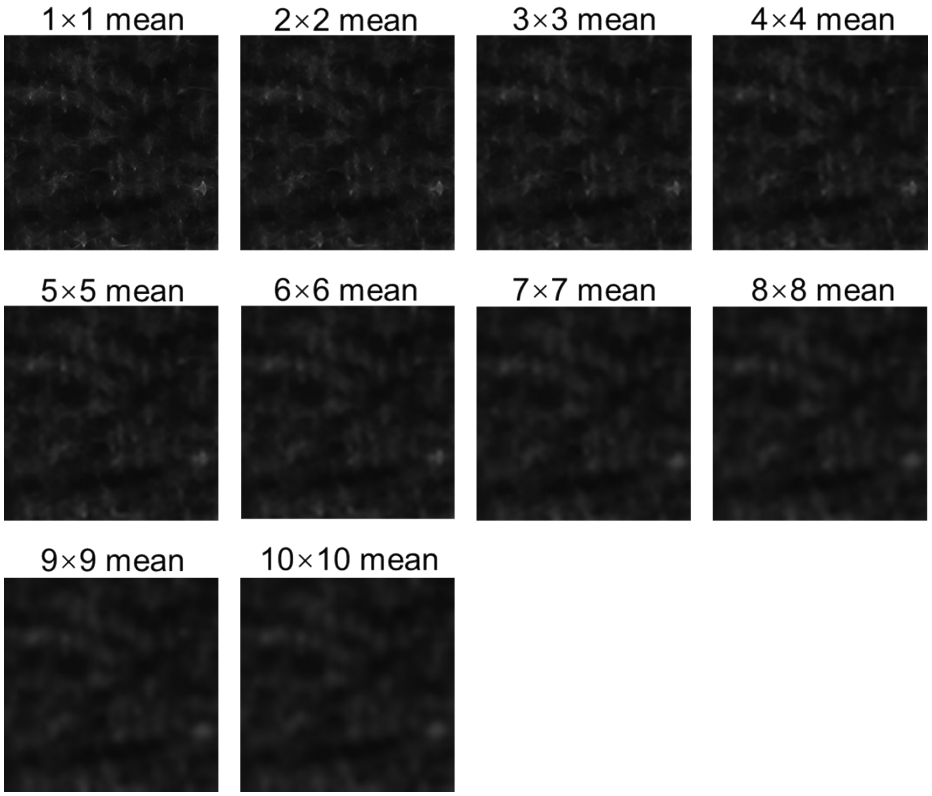

Figure S5. Images captured by the imaging module after averaging at different pixel levels.

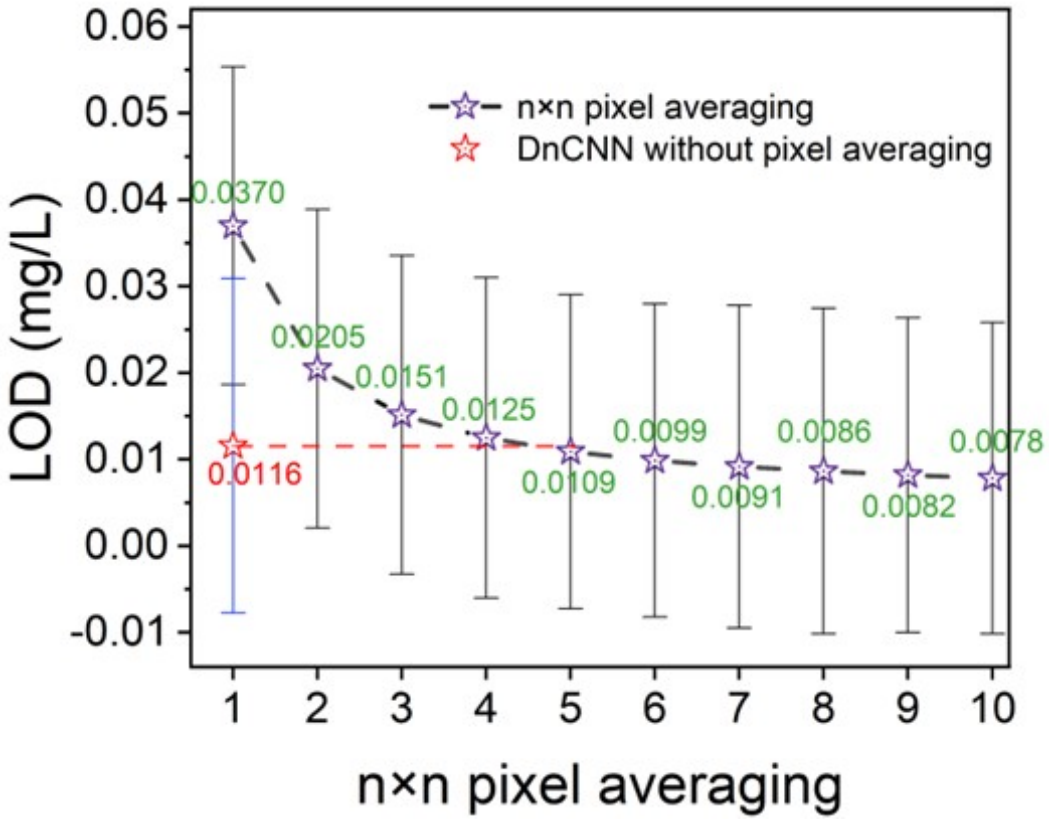

Figure S6. Schematic illustration with error bar of multi-pixel averaging for noise reduction in images.

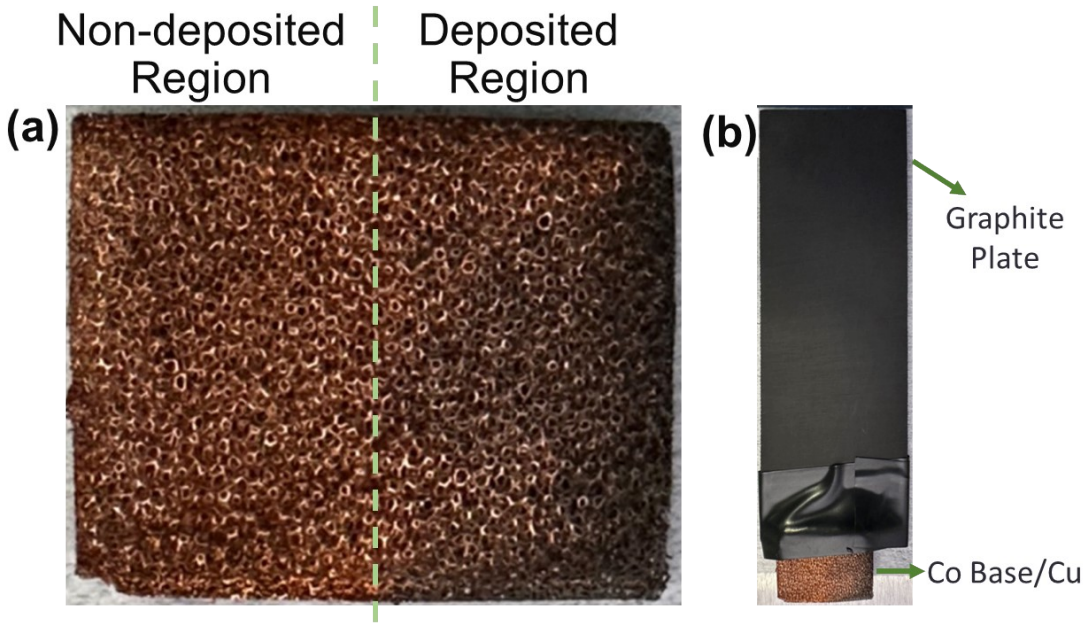

Figure S7. (a) The appearance of the homemade asymmetric Co Base/Cu. (b) The electrode fabricated by connecting the (Co Base/Cu) device to a high-purity graphite plate.

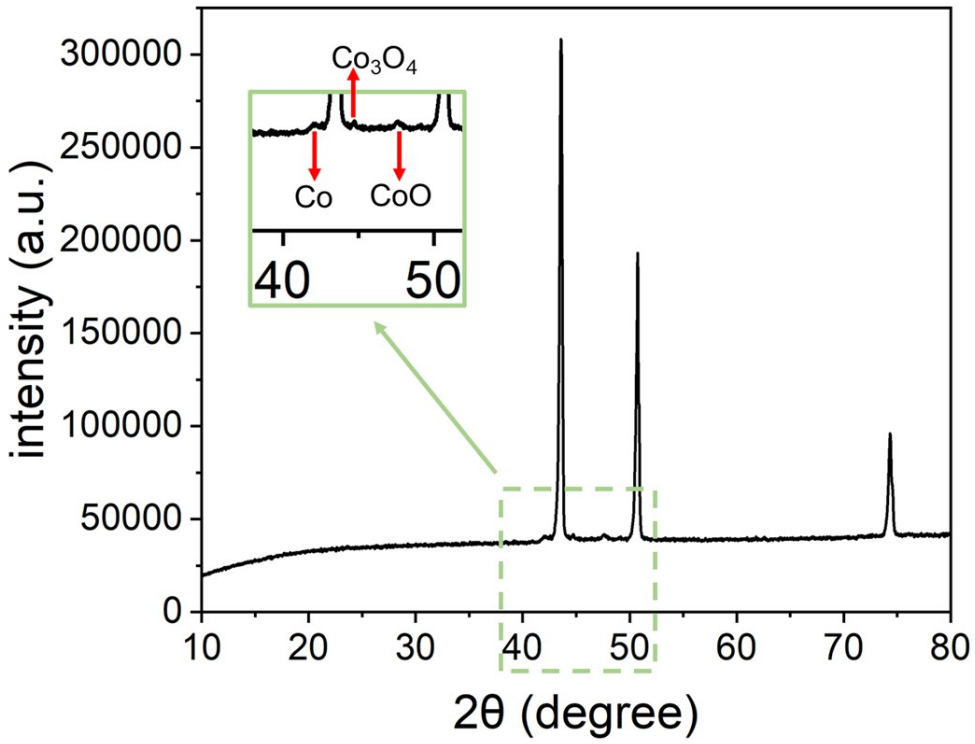

Figure S8. XRD patterns of the homemade asymmetric Co Base/Cu.

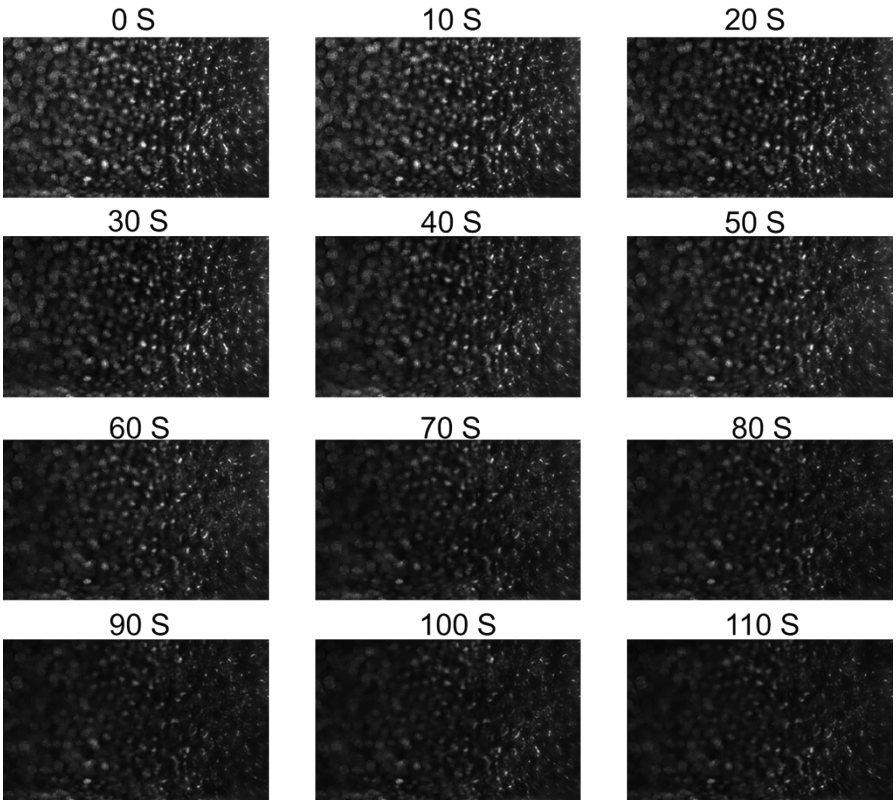

Figure S9. Images captured by the imaging module at different times when employing a self-made asymmetric Co Base/Cu electrode as the working electrode.

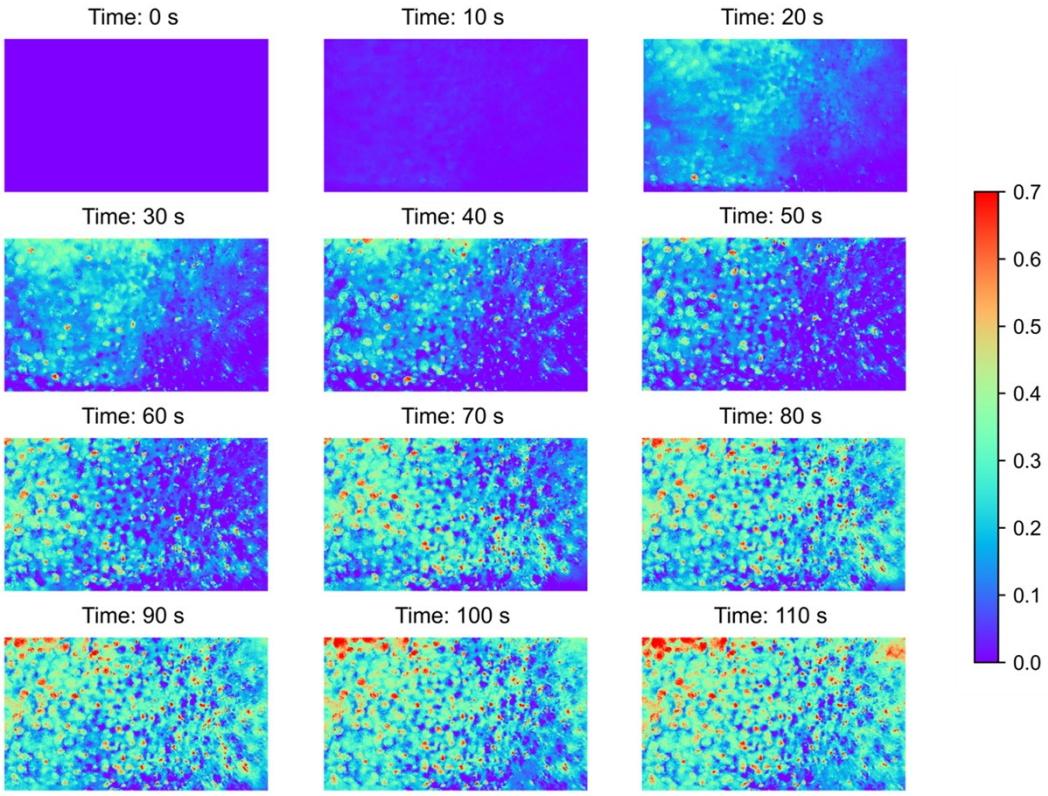

Figure S10. The distribution of nitrite concentrations at different times when employing a self-made asymmetric Co Base/Cu electrode as the working electrode.

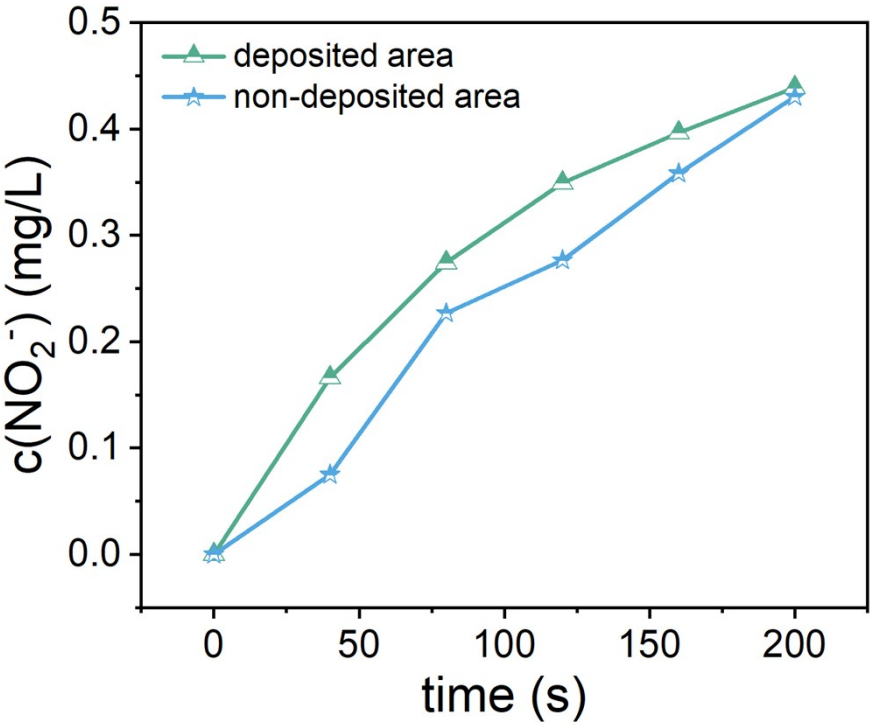

Figure S11. The change in concentration over time in both the deposited area and the non-deposited area when employing a self-made asymmetric Co Base/Cu electrode as the working electrode.